J Nanopart Res (2014) 16:2660
DOI 10.1007/s11051-014-2660-3

RESEARCH PAPER

Nitrogen-doped multi-walled carbon nanotubes modified with platinum, palladium, rhodium and silver nanoparticles in electrochemical sensing

Nikos G. Tsierkezos · Shereen Haj Othman · Uwe Ritter · Lars Hafermann · Andrea Knauer · J. Michael Köhler

Received: 20 June 2014 / Accepted: 17 September 2014 / Published online: 26 September 2014

Abstract Nitrogen-doped multi-walled carbon nanotubes (N-MWCNTs) were fabricated by means of chemical vapour deposition technique and decorated with platinum (PtNPs), palladium (PdNPs), rhodium (RhNPs) and silver (AgNPs) nanoparticles possessing diameter 2.7, 2.6, 2.7 and 3.4 nm, respectively. The electrochemical responses of composite films, further denoted as N-MWCNTs/MNPs (M: Pt, Pd, Rh and Ag) towards ferrocyanide/ferricyanide, $[Fe(CN)_6]^{3-/4-}$ were investigated in large concentration range (0.099–0.990 mM) in potassium chloride solution (1.0 M). The findings demonstrate that the electrochemical response and sensitivity of N-MWCNTs are improved significantly upon modification with metal nanoparticles. A strong dependence of film's electrochemical fineness on type of metal nanoparticles used for modification can be observed. Namely, the current response, the charge-transfer kinetics, and the detection capability of novel composite films enhance with the following order: N-MWCNTs < N-MWCNTs/RhNPs < N-MWCNTs/PdNPs < N-MWCNTs/PtNPs < N-MWCNTs/AgNPs. The findings demonstrate that the novel N-MWCNTs/MNPs composite films can be considered as powerful and useful materials for electrochemical sensing.

Keywords Electrochemical sensing · Metal nanoparticles · Multi-walled carbon nanotubes · Palladium · Platinum · Rhodium · Silver

Introduction

Multi-walled carbon nanotubes (MWCNTs) are very promising and attractive nanomaterials for various applications in electrochemistry due to their remarkable electrical, chemical and mechanical properties (Bernholc et al. 2002; Zhao et al. 2002; Dumitrescu et al. 2009). MWCNTs were extensively used for the production of novel sensors and the construction of precise devices, since they enhance the electron-transfer rate of redox systems and consequently, they improve the sensitivity of sensing techniques due to their large surface area and their high electrical conductivity (Luo et al. 2001; Musamech et al. 2002; Yu et al. 2007; Brahman et al. 2012). For instance, nanostructured carbon-based materials, such as

Electronic supplementary material The online version of this article (doi:10.1007/s11051-014-2660-3) contains supplementary material, which is available to authorized users.

N. G. Tsierkezos (✉) · S. Haj Othman · U. Ritter
Department of Chemistry, Institute of Chemistry and Biotechnology, Ilmenau University of Technology, Weimarer Straße 25, 98693 Ilmenau, Germany
e-mail: nikos.tsierkezos@tu-ilmenau.de

L. Hafermann · A. Knauer · J. M. Köhler
Department of Physical Chemistry and Micro Reaction Technology, Institute of Chemistry and Biotechnology, Ilmenau University of Technology, Gustav-Kirchhof Straße 1, 98693 Ilmenau, Germany

nitrogen-doped carbon nanotubes (N-MWCNTs), have shown quite respectable attractive electrochemical performance towards the oxygen reduction (Chung et al. 2013) and the oxidation of hydrogen peroxide (Xu et al. 2010). In addition, metal nanoparticles can serve as building blocks for the fabrication of advanced electrode materials. Specifically, metal nanoparticles allow the construction of sensors and electrochemical devices, with the possibility of controlling their selectivity, sensitivity and functionality, since they have tuneable optical and electronic properties. Namely, the optical, magnetic, electronic and catalytic properties of metal nanoparticles are strongly dependent on their morphology (size and shape) (Burda et al. 2005; Talapin et al. 2010). Thus, the fabrication of nanoparticles possessing different diameters and/or shapes results to species with various properties.

As was already reported in literature, metals with nanostructures, especially platinum, palladium, gold, silver and rhodium nanoparticles are of considerable interest for applications in catalysis, batteries, fuel cells, capacitors and electroanalytical biosensing (Attard et al. 1997; Wang and Agnes 1992; Xiao et al. 2003; Liu et al. 2000). However, there are some difficulties to use directly metal nanoparticles as material for working electrodes, and consequently, various approaches were developed to immobilize metal nanoparticles on the surface of appropriate substrates (Doron et al. 1995; Wang and Wang 2004). The supported substrates used for the immobilization of metal nanoparticles play a quite significant role, since they enhance the mechanical and thermal stability of metal nanoparticles and also maintain them in highly dispersed state (no agglomeration has to be occurred on surface of substrate) (Jarvi et al. 1997). Furthermore, to meet the requirement of transfer electron for electrochemical applications, the supported substrates should possess a relative great electrical conductivity. Therefore, N-MWCNTs can be considered as appropriate material to be applied as substrate for the deposition of metal nanoparticles.

In the present work, N-MWCNTs were fabricated and decorated with various metal nanoparticles. For the modification, PtNPs, PdNPs, RhNPs and AgNPs possessing diameters of approximately 3.0 nm were used. The effort to deposit the metal nanoparticles directly on the surface of carbon nanotubes was quite successful, and no agglomeration of nanoparticles was observed. The fabricated composite films, further denoted as N-MWCNTs/MNTs (M: Pt, Pd, Rh and Ag), were characterized electrochemically using the standard redox system $[Fe(CN)_6]^{3-/4-}$ by means of cyclic voltammetry and electrochemical impedance spectroscopy techniques. The findings demonstrate that the electrocatalytic activity of novel composite films towards $[Fe(CN)_6]^{3-/4-}$ tends to enhance with the following order: N-MWCNTs < N-MWCNTs/RhNPs < N-MWCNTs/PdNPs < N-MWCNTs/PtNPs < N-MWCNTs/AgNPs. The results extracted from the present work exhibit the importance of modifying N-MWCNTs for the improvement of their electrocatalytic properties.

Experimental section

Chemicals and solutions

Polyvinylpyrrolidone, 2-hydroxy-4′-(2-hydroxyethoxy)-2-methylpropiophenone, dihydrogen hexachloroplatinate, potassium hexacyanoferrate(III), potassium hexacyanoferrate(II) trihydrate, silver nitrate and potassium chloride were purchased from Sigma-Aldrich. Perfluoromethyldecalin, palladium(II) nitrate dehydrate and rhodium(III) chloride hydrate were purchased from F2 Chemicals Ltd., Carl Roth GmbH and Alfa Aesar GmbH & Co KG, respectively. All chemicals were used as received without any further purification. The solutions for the electrochemistry measurements were prepared by dilution of stock solution of $K_3Fe(CN)_6/K_4Fe(CN)_6$ (0.01 M) in 1.0 M aqueous KCl solution. The stock solution was prepared immediately prior to the electrochemical experiments using high-quality deionized water. The measured solutions in the concentration range of 0.099–0.990 mM were prepared directly in the electrochemical cell with progressive addition of an appropriate volume of the stock solution in 1.0 M aqueous KCl solution. The experiments were carried out at the room temperature.

Apparatus

All electrochemistry measurements were performed on electrochemical working station Zahner (IM6/6EX, Germany). The obtained results were analysed by means of Thales software (version 4.15). A three electrode system consisting of N-MWCNTs/MNPs

(M: Pt, Pd, Rh and Ag) working electrode, platinum auxiliary electrode and Ag/AgCl (saturated KCl) reference electrode was used for the measurements. The electrochemical impedance spectra were recorded in the frequency range from 0.1 Hz to 100 kHz at the half-wave potential of the studied redox system $[Fe(CN)_6]^{3-/4-}$ (+0.280 V vs. Ag/AgCl). All experiments were carried out at the room temperature. In all measurements, the solutions were deoxygenated by purging with high-purity nitrogen. More details regarding the electrochemical experiments were already reported in previous published article (Tsierkezos and Ritter 2011, 2012). The morphology and elemental composition of N-MWCNTs/MNPs (M: Pt, Pd, Rh and Ag) composite films were examined by scanning electron microscope FEI/Philips (model XL30 ESEM) equipped with an energy dispersive X-ray spectrometer (SEM/EDS).

Fabrication of N-MWCNTs/MNPs (M: Pt, Pd, Rh and Ag)

N-MWCNTs were synthesized by means of chemical vapour deposition technique onto oxidized porous silicon wafer using acetonitrile as carbon source material in the presence of ferrocene as catalyst. The fabrication process was performed in furnace at 900 °C using argon as carrier gas. The scheme of pyrolysis apparatus and more experimental details regarding the fabrication of N-MWCNTs were already reported in previous published articles (Szroeder et al. 2010; Tsierkezos and Ritter 2010). Colloidal noble metal nanoparticles were prepared using the photochemical segmented flow technique (Köhler et al. 2013). A representative scheme of apparatus used for the fabrication of metal nanoparticles is shown in Fig. 1. The apparatus consists of three PC-controlled syringe pumps, PTFE-tubing with an inner diameter of 0.5 mm, standard fluid connectors and one 4-port-manifold (both made of polyether ether ketone). The segmented flow technique is well suited for micro continuous-flow synthesis of plasmonic nanoparticles with high size homogeneity (Knauer et al. 2011, 2012) and for tuning of nanoparticle properties (Knauer and Köhler 2013). It causes a narrow residence time distribution for all volume elements of the reactant mixture under the UV ray and a high reproducibility of the fluid motion in this range. All noble metal nanoparticles were prepared using the corresponding metal salt solutions (1.0 mM). The salt solution was mixed with the polyvinylpyrrolidone/photoinitiator solution (PVP/PI) in a 4-port-manifold and segmented with perfluoromethyldecalin (PP9). The PVP/PI solution was previously prepared from PVP solution (2 wt%) and 2-hydroxy-4′-(2-hydroxyethoxy)-2-methylpropiophenone solution (1.0 mM). The nucleation starts with the irradiation of the segments in the photo initiation element (2 mm length of the focus, irradiation time: 135 ms). The properties of the synthesized metal nanoparticles, such as the particles diameter, the full width at half maximum and the particles number are reported in Table 1. The diagrams showing the size distribution of the fabricated metal nanoparticles are shown in Figs. S1–S4 (Supplementary material). From the values reported in Table 1, it can be clearly seen that AgNPs possess the greatest diameter as well as the greatest number of particles from all studied metal nanoparticles.

The N-MWCNTs films were decorated with MNPs (M: Pt, Pd, Rh and Ag) according to the following procedure: the N-MWCNTs films were immersed in aqueous solution of sodium citrate (2.5 mM) and left in solution for about 10 min. After the treatment, the films were dried in the air for about 120 min at the room temperature. Afterwards, MNPs (M: Pt, Pd, Rh and Ag) were dropped onto treated N-MWCNTs films using a micropipette and let for drying under room conditions. Finally, the composite films were carefully washed with distilled water and dried in the air for about 24 h. In order to construct the N-MWCNTs/MNPs (M: Pt, Pd, Rh and Ag) working electrodes for the electrochemical measurements, the films were connected to copper wire using silver conducting coating (silver paint). Once the silver coating was dried (after about 24 h), the silver conducting part of the films was fully covered with varnish protective coating (nail enamel). As soon as the varnish protective coating was dried (after about 12 h), the films were ready to be used for the electrochemical measurements. It must be stated that the fabricated N-MWCNTs/MNPs (M: Pt, Pd, Rh and Ag) composite films were quite stable and no detachment of electrode's contacting occurred during the measurements.

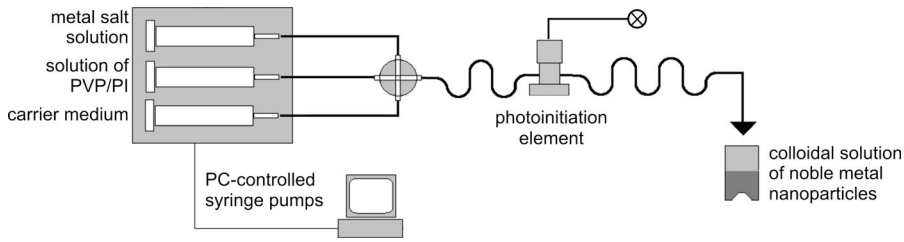

Fig. 1 Scheme of apparatus used for the fabrication of metal nanoparticles

Table 1 Properties of metal nanoparticles used for the decoration of N-MWCNTs

Parameter	RhNPs	PdNPs	PtNPs	AgNPs
Particles diameter (nm)	2.7	2.6	2.7	3.4
Full width at half maximum (nm)	1.7	1.4	1.5	1.5
Particles number (ml^{-1})	3.4×10^{13}	2.4×10^{13}	3.1×10^{13}	4.9×10^{13}

Results and discussion

Morphology of N-MWCNTs/MNPs (M: Pt, Pd, Rh and Ag)

The SEM micrographs taken for unmodified N-MWCNTs exhibit that the film's surface is quite homogeneous. The fabricated films consist of aligned carbon nanotubes with rather enhanced arrangement, which contain great amount of incorporated nitrogen into their structure. It is well known that upon decomposition of acetonitrile nitrogen-doped carbon nanotubes are formed. TEM micrographs taken for N-MWCNTs demonstrate that the carbon nanotubes possess the so-called bamboo structure that is quite common for multi-walled carbon nanotubes, which incorporate nitrogen into their structure (nitrogen-doped carbon nanotubes). The thickness of fabricated N-MWCNTs films was estimated to vary in range from 26 to 28 μm. SEM and TEM images of N-MWCNTs substrate were already published in previous articles (Szroeder et al. 2010). The SEM images taken for N-MWCNTs/MNPs (M: Pt, Pd, Rh and Ag) films reveal that the deposited metal nanoparticles are dispersed homogenously onto the surface of N-MWCNTs and that no agglomeration of nanoparticles takes place. It is interesting that the modified with metal nanoparticles films demonstrate quite net structure, which is quite favourable for electron-transfer processes. This evidence is reflected by the greater active surface area of modified films compared to that of unmodified N-MWCNTs. Specifically, it has been observed that the electro-active area of N-MWCNTs film can be increased up to more than 70 % upon modification of nanotubes with metal nanoparticles (see "Electrochemical applications of N-MWCNTs/MNPs (M: Pt, Pd, Rh and Ag)" section). Representative SEM images taken for the fabricated N-MWCNTs/MNPs (M: Pt, Pd, Rh and Ag) are shown in Fig. 2. The SEM images were taken with an accelerating voltage of 2.0 kV and magnification factors in the range from 70,000 to 180,000. The metal nanoparticles can be recognized in SEM micrographs as small bright dots deposited on the outer walls of carbon nanotubes.

Electrochemical applications of N-MWCNTs/MNPs (M: Pt, Pd, Rh and Ag)

Representative CVs recorded for the standard redox system $[Fe(CN)_6]^{3-/4-}$ (1.0 M KCl) on either unmodified N-MWCNTs or modified N-MWCNTs/MNPs (M: Pt, Pd, Rh and Ag) composite films showing the effect of change of concentration of redox system on anodic current density are shown in Figs. S5–S9 (Supplementary material). For comparison reasons, CVs recorded for a single concentration of $[Fe(CN)_6]^{3-/4-}$ (0.990 mM) onto unmodified N-MWCNTs and modified N-MWCNTs/MNPs (M: Pt, Pd, Rh and Ag) films are shown in Fig. 3. The electrochemical parameters extracted for the interpretation of recorded CVs are reported in Table 2. On unmodified N-MWCNTs and modified N-MWCNTs/MNPs films quite symmetrical CVs were recorded that

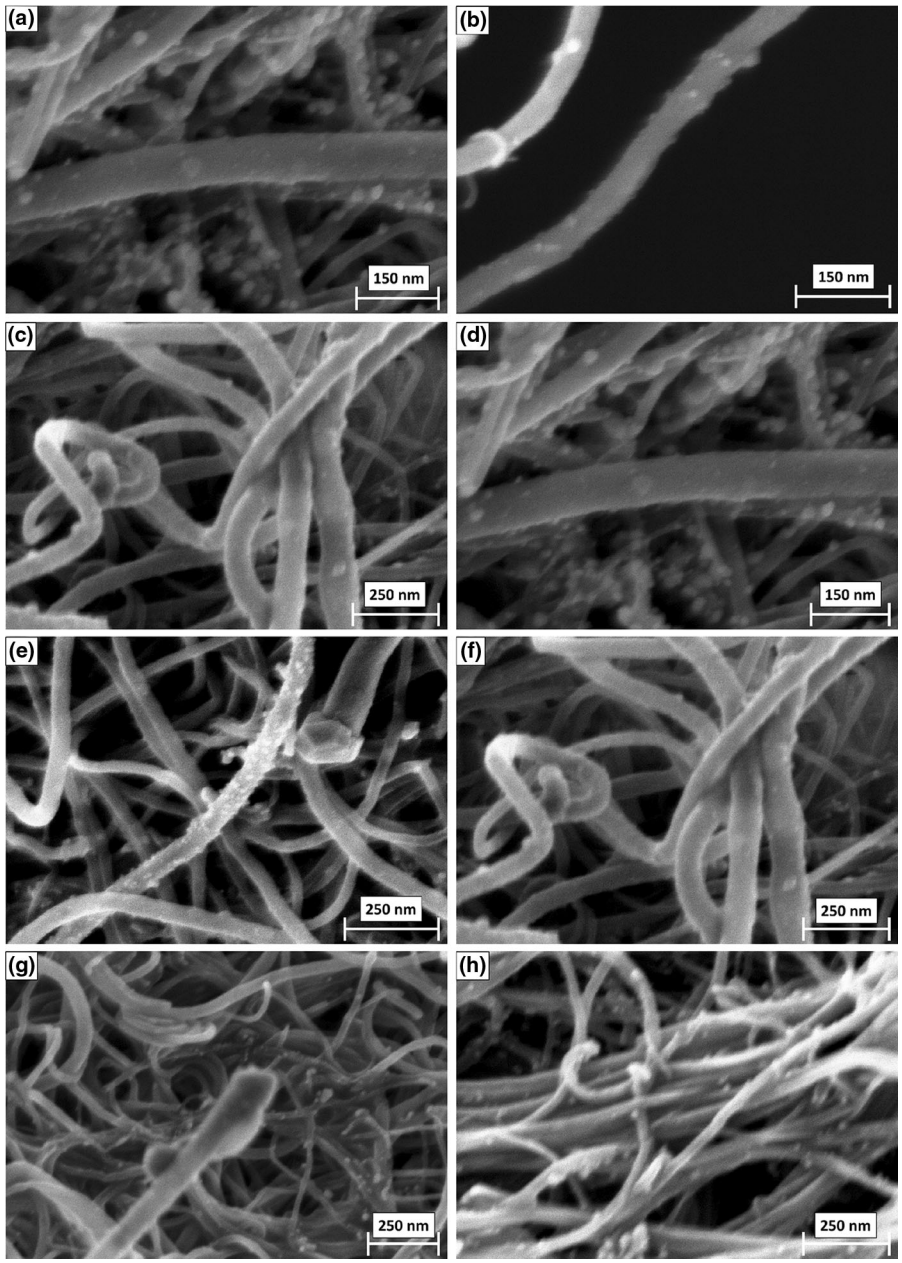

Fig. 2 SEM micrographs taken for N-MWCNTs/AgNPs (**a**, **b**), N-MWCNTs/PtNPs (**c**, **d**), N-MWCNTs/PdNPs (**e**, **f**), and N-MWCNTs/RhNPs (**g**, **h**) composite films

consist of an oxidation wave in the range of 0.31–0.32 V (vs. Ag/AgCl), corresponding to one-electron oxidation of $[Fe^{II}(CN)_6]^{4-}$ to $[Fe^{III}(CN)_6]^{3-}$, and reduction wave in the range of 0.24–0.25 V (vs. Ag/AgCl), representing the inverse process, namely the reduction of $[Fe^{III}(CN)_6]^{3-}$ to $[Fe^{II}(CN)_6]^{4-}$. The recorded CVs demonstrate that the redox couple $[Fe(CN)_6]^{3-/4-}$ tends to be reversible on both types of films (unmodified and modified), but nevertheless, some slight kinetic differences for electron-transfer process can be recognized on the shape of recorded CVs. It is nevertheless interesting to mention that in all studied unmodified and modified N-MWCNTs-based films slight shift of oxidation and reduction peaks to

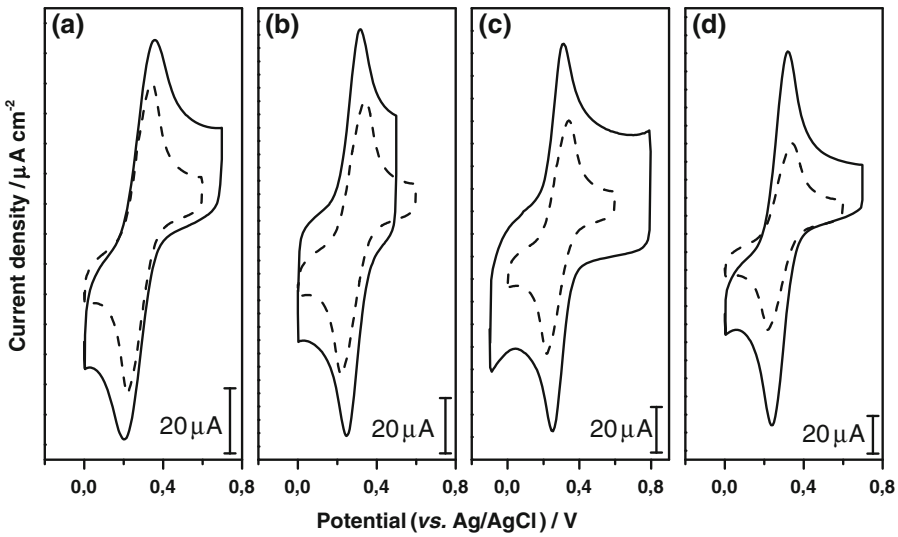

Fig. 3 CVs recorded for 0.990 mM $[Fe(CN)_6]^{3-/4-}$ (1.0 M KCl) on N-MWCNTs/RhNPs (**a**), N-MWCNTs/PdNPs (**b**), N-MWCNTs/PtNPs (**c**), N-MWCNTs/AgNPs (**d**) composite films at the scan rate of 0.02 V s^{-1}. For comparison reasons the CVs recorded for 0.990 mM $[Fe(CN)_6]^{3-/4-}$ (1.0 M KCl) on N-MWCNTs composite film (*dashed line*) are also included

more positive and less positive potentials, respectively, were observed with the increase of concentration of studied redox system $[Fe(CN)_6]^{3-/4-}$. Consequently, the anodic and cathodic peak potential separation ($\Delta E_p = E_p^{ox} - E_p^{red}$) tends to increase with the rise in concentration of redox system. Since the slow electron-transfer kinetic is independent of concentration of redox system, while the effect of uncompensated resistance of electrochemical cell dependents on concentration, the findings reveal that the shift of oxidation and reduction potentials, and thus, the variation of peak potential separation with the change of concentration of redox system is due to cell resistance that remains uncompensated (it must be mentioned that only a part of resistance was compensated during the measurements). In both types of N-MWCNTs films (unmodified and modified), the peak current ratio of reverse and forward scans is equal to unity (within experimental error) and is independent of the scan rate applied for recording the CVs indicating that there are no parallel chemical reactions coupled to electrochemical process. Furthermore, the oxidative and reductive peak currents are essentially constant for large number of cycles, demonstrating that there are no chemical reactions coupled with the electron transfer and confirming that the studied electro-active species are stable in the time frame of the experiment and that the charge-transfer process occurring on studied composite films is reversible. The half-wave potential ($E_{1/2}$) of $[Fe(CN)_6]^{3-/4-}$ estimated as the average value of oxidation and reduction potentials was constant within experimental error on both types (unmodified and modified) of composite films ($E_{1/2} = +0.280$ V vs. Ag/AgCl), something that is expectable for reversible redox systems.

Considering that the anodic and cathodic peak potential separation (ΔE_p) varies inversely with the heterogeneous electron-transfer rate constant (k_s), and consequently, with the kinetics of charge-transfer process occurring onto composite films, some interesting remarks can be extracted from recorded CVs. Specifically, the CVs exhibit that some small differences for electron-transfer kinetics occur on various composite films studied. Namely, the anodic and cathodic peak potential separation (ΔE_p) obtained on unmodified N-MWCNTs film ($\Delta E_p \approx 0.083$ V) appears to be greater compared to the theoretical ΔE_p that is suggested for one-electron-transfer process ($\Delta E_p \approx 0.059$ V) (Lu et al. 2005) demonstrating slight deviation of $[Fe(CN)_6]^{3-/4-}$ from reversibility on this particular electrode. Nevertheless, it is amazing that on N-MWCNTs films decorated with PdNPs, PtNPs and AgNPs, the ΔE_p values of 0.062, 0.060 and 0.059 V were determined, respectively, that lie within experimental error very close to the expected theoretical ΔE_p value. These findings demonstrate an improvement of kinetics of electron transfer onto N-MWCNTs films decorated with this type of metal nanoparticles. In contrast to the other modified N-MWCNTs/MNPs electrodes, the N-MWCNTs film modified with RhNPs exhibits greater ΔE_p value ($\Delta E_p \approx 0.078$ V) indicating a slight declining of

Table 2 Anodic peak potential (E_p^{ox}), cathodic peak potential (E_p^{red}), half-wave potential ($E_{1/2}$), peak potential separation (ΔE_p), active surface area (A), anodic peak current density (i_p^{ox}), anodic and cathodic peak current ratio (i_p^{ox}/i_p^{red}), heterogeneous electron-transfer rate constant (k_s), charge-transfer resistance (R_{ct}), lower limit of detection (*LOD*), and sensitivity (S) of $[Fe(CN)_6]^{3-/4-}$ (1.0 M KCl) on N-MWCNTs and N-MWCNTs/MNPs (M: Rh, Pd, Pt and Ag) composite films

Parameter	N-MWCNTs		N-MWCNTs/MNPs		
	Unmodified	RhNPs	PdNPs	PtNPs	AgNPs
E_p^{ox} (V[a])	0.321	0.319	0.311	0.310	0.309
E_p^{red} (V[a])	0.238	0.241	0.249	0.250	0.250
$E_{1/2}$ (V[b])	0.280	0.280	0.280	0.280	0.280
ΔE_p (V)	0.083	0.078	0.062	0.060	0.059
A (cm^2)	3.93	5.56	6.10	6.37	6.96
i_p^{ox} ($\mu A\ cm^{-2}$)	49	65	78	90	101
i_p^{ox}/i_p^{red}	1.01	1.00	1.01	0.98	1.00
k_s (10^{-2} cm s^{-1})[c]	0.51	0.77	3.61	4.49	5.03
k_s (10^{-2} cm s^{-1})[d]	0.62	1.41	3.04	4.22	6.98
R_{ct} (Ω)[e]	58	43	12	10	2
LOD (μM)[f]	0.341	0.232	0.185	0.157	0.138
S (A M^{-1} cm^{-2})	0.464	0.603	0.696	0.766	0.836

[a] All potentials are reported with respect the Ag/AgCl (KCl sat.) reference electrode

[b] The $E_{1/2}$ values were determined as the average values of E_p^{ox} and E_p^{red}

[c] The k_s values were determined from electrochemical absolute rate relation: $\psi = (D_o/D_R)^{a/2}k_s(n\pi F v D_o/RT)^{-1/2}$, where ψ is kinetic parameter, a the charge-transfer coefficient ($a \approx 0.5$), D_o, D_R the diffusion coefficients of oxidized and reduced species, respectively ($D_o \approx D_R$), and n the number of electrons involved in the redox reaction ($n = 1$) (Nicholson 1965)

[d] The k_s values were determined from EIS parameters according to relation: $R_{ct} = RT/n^2F^2Ak_sc$, where R_{ct} is the charge-transfer resistance, A the active surface area, and c the concentration of redox system (Galus 1994)

[e] The EIS parameters were determined using the equivalent electrical circuit ($R_s + (C_{dl}/(R_{ct} + Z_w))$) (software Thales, version 4.15)

[f] The detection limits were estimated on the basis of signal-to-noise (S/N) ratio of 3 by means of CV technique

electron-transfer kinetics onto this particular composite electrode. It is, however, interesting that on N-MWCNTs/RhNPs smaller ΔE_p value was obtained compared to that on unmodified N-MWCNTs demonstrating that the kinetics of electron transfer for redox process tends to be improved upon modification of N-MWCNTs with metal nanoparticles. Since the peak potential separation varies inversely with the kinetics of charge-transfer process, it is expected that the rate of the redox process involving $[Fe(CN)_6]^{3-/4-}$ on novel composite films increases with the order: N-MWCNTs < N-MWCNTs/RhNPs < N-MWCNTs /PdNPs < N-MWCNTs/PtNPs < N-MWCNTs/AgNPs. The heterogeneous electron-transfer rate constants were estimated by means of electrochemical absolute rate relation that is based on degree of peak potential separation between the forward and reverse scans. Namely, the heterogeneous electron-transfer rate constants of $[Fe(CN)_6]^{3-/4-}$ on unmodified N-MWCNTs and modified N-MWCNTs/MNPs (M: Pt, Pd, Rh and Ag) films were determined by means of Nicholson procedure (Nicholson 1965) which relates k_s with ΔE_p through a working curve of the dimensionless kinetic parameter ψ. It must be mentioned; however, that only approximate k_s values can be estimated by means of electrochemical absolute rate equation since this relation is limited to planar diffusion flat electrodes something that is not correct in the present work where carbon nanotubes-based film with relative hard and rough surface was used. Furthermore, the small amount of cell resistance that remains uncompensated affects slightly the peak-to-peak potential separation and therefore the rate of charge transfer. For the determination of k_s, the diffusion coefficient value of $D = 7.26 \times 10^{-6}$ cm^2 s^{-1} was considered for $[Fe(CN)_6]^{3-/4-}$ (Konopka and McDuffie 1970). The determined k_s values are included in Table 2. In addition, the k_s values of $[Fe(CN)_6]^{3-/4-}$ on various studied composited films

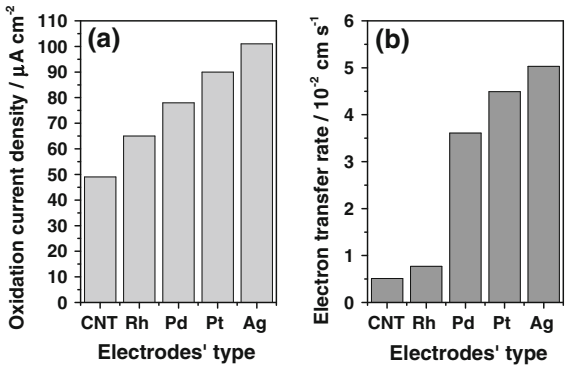

Fig. 4 Histograms showing the oxidation current density (**a**) and the heterogeneous electron-transfer rate constant (**b**) of 0.990 mM $[Fe(CN)_6]^{3-/4-}$ (1.0 M KCl) on N-MWCNTs (symbolized in diagram as CNT) and N-MWCNTs/MNPs (M: Rh, Pd, Pt and Ag) composite films (symbolized in diagram as Rh, Pd, Pt and Ag)

are presented in histogram in Fig. 4b. As was expected, the k_s value of $[Fe(CN)_6]^{3-/4-}$ onto composite N-MW CNTs films modified with various metal nanoparticles varies inversely with the peak potential separation. Specifically, the highest rate for electron transfer for $[Fe(CN)_6]^{3-/4-}$ was observed on N-MWCNTs/AgNPs, which exhibits the lowest ΔE_p, while onto unmodified N-MWCNTs film having the greatest ΔE_p value rather low rate for electron transfer for $[Fe(CN)_6]^{3-/4-}$ was estimated. Namely, the rate for electron transfer of $[Fe(CN)_6]^{3-/4-}$ on various composite films increases with the order: N-MWCNTs < N-MWCNTs/RhNPs < N-MWCNTs/PdNPs < N-MWCNTs/PtNPs < N-MW CNTs/AgNPs. It is very interesting that the findings reveal that upon modification of N-MWCNTs with RhNPs, PdNPs, PtNPs and AgNPs the rate for electron transfer of $[Fe(CN)_6]^{3-/4-}$ increases for about ~50, ~608, ~780 and ~886 %, respectively, compared to that of unmodified N-MWCNTs film. These findings demonstrate the important effect of the modification of N-MWCNTs-based films with metal nanoparticles on improvement of film's electrochemical response. It is amazing that the k_s values of $[Fe(CN)_6]^{3-/4-}$ estimated in present work on N-MWCNTs/MNPs composite films appear to be significantly greater (in some cases up to 15 times greater) compared to those reported in literature for the same redox system on either bare gold ($k_s \approx 0.26 \times 10^{-2}$ cm s^{-1}) or modified gold electrode ($k_s \approx 0.29 \times 10^{-2}$ cm s^{-1}) (He et al. 2005).

The CV results exhibit that an obvious improvement of electrochemical current response of N-MWCNTs films towards $[Fe(CN)_6]^{3-/4-}$ occurs with their modification with metal nanoparticles. Consequently, the anodic and cathodic current density of modified with metal nanoparticles films appear to be greater compared to that of unmodified N-MWCNTs film (measured for the same concentration of redox system). It is evident that the metal nanoparticles provide the required conduction pathways facilitating the redox process. It is also possible that the metal nanoparticles attached on surface of N-MWCNTs films increase significantly the effective surface area of the electrodes, and thus, improve their amperometric response. As it can be seen in Table 2, the effective surface area of unmodified N-MWCNTs film (with geometrical area of 1.0 cm^2), increases for about 41, 55, 62 and 77 %, upon its modification with RhNPs, PdNPs, PtNPs and AgNPs, respectively. It is very interesting that some small differences in amperometric responses of N-MWCNTs films were observed upon their modification with the various metal nanoparticles. Namely, with the modification of N-MWCNTs films with RhNPs an increase of about 33 % is observed in anodic current density compared to unmodified films. A modification of the N-MWCNTs films with PdNPs results to an improvement of anodic current density of about 59 %, while the decoration of N-MWCNTs with PtNPs leads to an enhancement of oxidation peak current density of about 84 %. Finally, upon modification of N-MWCNTs film with AgNPs an improvement of the oxidation current density of about 106 % occurs. These findings demonstrate that with the modification of the films with metal nanoparticles the amperometric response of composite films towards $[Fe(CN)_6]^{3-/4-}$ enhances since the electron transfer between the analyte and the electrode surface is promoted. The anodic current density of $[Fe(CN)_6]^{3-/4-}$ redox system onto unmodified and modified with metal nanoparticles N-MWCNTs films is presented graphically in histogram in Fig. 4a.

The oxidation peak current density for unmodified and modified with metal nanoparticles N-MWCNTs films towards $[Fe(CN)_6]^{3-/4-}$ investigated in concentration range of 0.099–0.990 mM by means of CV technique was found to be linear, permitting, thus, the determination of film's lower limit of detection and sensitivity. The estimated values of detection limit and sensitivity are included in Table 2. Furthermore, the values of limit of detection and sensitivity of

N-MWCNTs and N-MWCNTs/MNPs (M: Pt, Pd, Rh and Ag) composite films towards $[Fe(CN)_6]^{3-/4-}$ are presented in histograms in Fig. 5a, b, respectively. As it can be seen in histograms an improvement of the detection capability of the N-MWCNTs films with their modification with metal nanoparticles occurs. Namely, the findings exhibit that the limit of detection and the sensitivity of N-MWCNTs films towards $[Fe(CN)_6]^{3-/4-}$ are improved significantly upon their modification with metal nanoparticles. It is very interesting that within the nanoparticles investigated, AgNPs appears to improve significantly the film's electrocatalytic activity. Furthermore, the capability of RhNPs to enhance the film's electrocatalytic activity can be considered restricted, compared to the other studied metal nanoparticles (compared to unmodified N-MWCNTs film the detection capability of N-MWCNTs/RhNPs is great). Specifically, upon modification of N-MWCNTs with RhNPs, PdNPs, PtNPs and AgNPs an improvement of film's detection capability of about 32, 46, 54 and 60 %, respectively, occurs. Furthermore, the sensitivity of N-MWCNTs film towards $[Fe(CN)_6]^{3-/4-}$ enhances for about 29, 50, 65 and 80 % with its decoration with RhNPs, PdNPs, PtNPs and AgNPs, respectively (Table 2). These findings exhibit the important role that plays the nature of attached metal nanoparticles on film's electrochemical response. It would be very interesting to compare the limits of detection of N-MWCNTs/MNPs (M: Pt, Pd, Rh and Ag) towards $[Fe(CN)_6]^{3-/4-}$ with those reported in literature for other novel composite films. In general, the comparison demonstrates that the MWCNTs/MNPs (M: Pt, Pd, Rh and Ag) films exhibit greater detection ability (lower detection limit) towards $[Fe(CN)_6]^{3-/4-}$ compared to other novel electrodes reported in literature. For instance, the detection limit of 100 μM reported for carbon paste electrode modified with 1-butyl-4-methylpyridinium tetrafluoroborate towards $[Fe(CN)_6]^{3-/4-}$ (Pandurangachar et al. 2010) seems to be significantly poorer compared to that obtained on our N-MWCNTs/MNPs films. In addition, the detection limit of 100 μM reported for carbon paste electrode modified with sodium dodecyl sulphate towards $[Fe(CN)_6]^{3-/4-}$ (Niranjana et al. 2009) is likewise considerably poorer compared to that measured on our N-MWCNTs/MNPs. Furthermore, the detection limit of 30 μM reported for glass capillary ultra-microelectrode towards $[Fe(CN)_6]^{3-/4-}$ (Hirano et al. 2001) seems to be noticeably poorer compared to that measured on our novel N-MWCNTs/MNPs. Besides, the detection limit of glassy carbon electrode

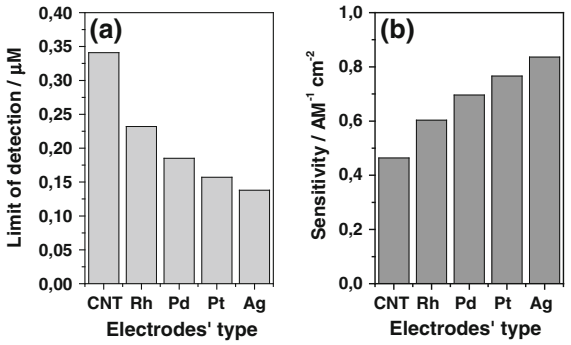

Fig. 5 Histograms showing the lower limit of detection (**a**) and the sensitivity (**b**) of N-MWCNTs (symbolized in diagram as CNT) and N-MWCNTs/MNPs (M: Rh, Pd, Pt and Ag) composite films (symbolized in diagram as Rh, Pd, Pt and Ag) towards $[Fe(CN)_6]^{3-/4-}$ (1.0 M KCl)

modified with titan dioxide and MWCNTs towards $[Fe(CN)_6]^{3-/4-}$ was reported as 48.6 and 1.10 μM (Perenlei et al. 2011), which appears to be also significantly poorer compared to that measured on our N-MWCNTs/MNPs. From this comparison, it can be clearly seen that the detection capability of N-MWCNTs/MNPs (M: Pt, Pd, Rh and Ag) films appears to be obviously better compared to other composite films reported in literature. These results demonstrate the excellent response of N-MWCNTs-based films "decorated" with metal nanoparticles.

The electrochemical impedance spectroscopy (EIS) technique is a valuable analytical tool for the investigation of electrical properties of composite films (Roto and Villemure 2002; Barreira et al. 2004). Consequently, in the present work, electrochemical impedance spectra were recorded in the whole investigated concentration range of 0.099–0.990 mM in order to estimate the barrier for electron transfer occurring on N-MWCNTs/MNPs (M: Pt, Pd, Rh and Ag) films. Representative EIS spectra recorded for 0.990 mM $[Fe(CN)_6]^{3-/4-}$ (1.0 M KCl) on N-MWCNTs and N-MWCNTs/MNPs (M: Pt, Pd, Rh and Ag) composite films are shown in Fig. 6. EIS spectra recorded for various concentrations of $[Fe(CN)_6]^{3-/4-}$ (1.0 M KCl) on N-MWCNTs and N-MWCNTs/MNPs (M: Pt, Pd, Rh and Ag) films along with the estimated (simulated) charge-transfer resistances are shown in Figs. S10–S14 (Supplementary material). The recorded EIS spectra (presented as Nyquist plots) have the shape of characteristic impedance spectrum, namely they include a part of

depressed semicircle followed by a straight line. The depressed semicircle, observed at higher frequencies (it is almost not observable), corresponds to the electron-transfer limited process, whereas the linear part that can be seen in lower frequencies represents the diffusion limited electron-transfer process. It is well known that in case of very fast electron-transfer process, the EIS spectrum includes only the linear part, whereas very slow electron-transfer procedure results to semicircle with a great diameter that is not accompanied by a straight line. As it can be seen in EIS spectra shown in Fig. 6, on studied N-MWCNTs/MNPs composite films the linear part prevails over the semicircle (only a small part of depressed semicircle can be seen in high-frequency region of EIS spectrum), indicating that the electron-transfer process occurring on N-MWCNT/MNPs composite films is quite fast (reversible Nernstian process). In contrast, on unmodified N-MWCNTs film an obvious semicircle can be recognized in high-frequency region of the spectrum indicating that a limited electron-transfer process takes place onto this particular electrode. For the simulation of the recorded EIS spectra, the equivalent electrical circuit of $(R_s + (C_{dl}/(R_{ct} + Z_w)))$ was used (Fig. S15, Supplementary material). The circuits' elements can be explained as follows: R_s is the solution resistance, C_{dl} the double layer capacitance (constant phase element was used instead of capacitor), R_{ct} the charge-transfer resistance and Z_w the Warburg diffusion impedance (Pauliukaite et al. 2010). The most suitable impedance parameter for studying the interfacial properties of modified films is the charge-transfer resistance (R_{ct}). This parameter controls the electron-transfer kinetics of redox system at electrode interface and represents the barrier for the electron-transfer process (the hindering behaviour of interface properties of composite film). In the present work, it was observed that the charge-transfer resistance increases slightly with the rise of the concentration of electro-active substance. This observation that is more obvious on unmodified N-MWCNTs can be connected to the interruption of the electron-transfer process caused by the uncompensated resistance effect, which becomes more significant with increase of concentration of the electro-active substance.

The findings clearly demonstrate that with the modification of N-MWCNTs films with metal nanoparticles the charge-transfer resistance decreases indicating faster interfacial electron transfer onto modified with MNPs films compared to unmodified N-MWCNTs film. It is very interesting that with the modification of N-MWCNTs with metal nanoparticles a significant decrease of R_{ct} occurs that in some cases appears to be more than 90 % (Table 2). Namely, upon modification of N-MWCNTs films with RhNPs, PdNPs, PtNPs and AgNPs the film's charge-transfer resistance decreases for about 26, 79, 83 and 97 %, respectively. It is, consequently, obvious that the metal nanoparticles promote the electron transfer between the analyte and the electrode surface due to the smaller electron-transfer barrier introduced with the modification of N-MWCNTs with metal nanoparticles. From the impedance parameters, the k_s values of $[Fe(CN)_6]^{3-/4-}$ redox system on N-MWCNTs/MNPs composite films were once more estimated and are included in Table 2. The charge-transfer resistances along with the estimated electron-transfer rate constants are presented in histograms in Fig. S16 (Supplementary material). As it can be seen in Table 2, the k_s values estimated by means of EIS technique differ somewhat from those approximated by means of electrochemical absolute rate relation. This disagreement can be attributed to the greater inaccuracy of calculating k_s by means of electrochemical absolute rate relation (because of the hardness and roughness of the films as well as the effect of uncompensated resistance). However, the variation of k_s with the type of metal nanoparticles has the same trend, namely the findings demonstrate that within the metal nanoparticles studied, AgNPs seem to be the greatest electrocatalyst (faster kinetic for electron transfer), while the electrocatalytic activity of RhNPs appears to be limited (lowest kinetic for electron transfer). The findings are in absolute accordance with the extracted CV results, where an improvement of electron-transfer rate constant and films' detection capability towards $[Fe(CN)_6]^{3-/4-}$ was observed with the order: N-MWCNTs < N-MWCNTs/RhNPs < N-MWCNTs/PdNPs < N-MWCNTs/PtNPs < N-MWCNTs/AgNPs. It would be very interesting to compare the impedance results obtained in the present work for $[Fe(CN)_6]^{3-/4-}$ on N-MWCNTs/MNPs (M: Pt, Pd, Rh and Ag) films with those reported in literature for conventional electrodes and other novel films modified with metal nanoparticles. Li and Chen (2012) reported for $[Fe(CN)_6]^{3-/4-}$ (PBS, pH 7.0) on bare glassy carbon electrode a charge-transfer resistance of 1.91 kΩ that is greater compared to that obtained in the present work on either unmodified N-MWCNTs or modified N-MW

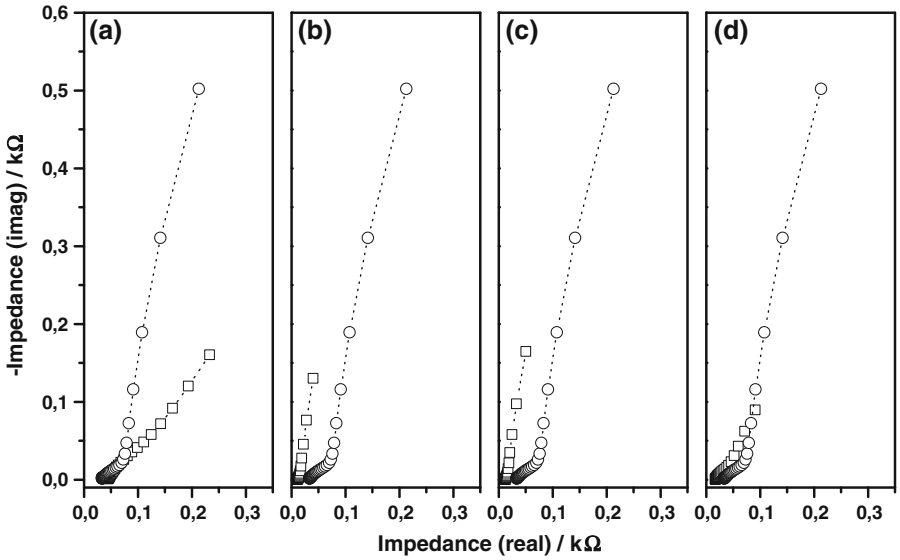

Fig. 6 EIS spectra recorded for 0.990 mM $[Fe(CN)_6]^{3-/4-}$ (1.0 M KCl) on N-MWCNTs/RhNPs (**a**) (*open square*), N-MWCNTs/PdNPs (**b**) (*open square*), N-MWCNTs/PtNPs (**c**) (*open square*), and N-MWCNTs/AgNPs (**d**) (*open square*) composite films. The EIS spectra were recorded at the half-wave potential of $[Fe(CN)_6]^{3-/4-}$ (+0.280 V vs. Ag/AgCl) in the frequency range from 0.1 Hz to 100 kHz. For comparison reasons, the EIS spectra recorded for 0.990 mM $[Fe(CN)_6]^{3-/4-}$ (1.0 M KCl) on N-MWCNTs (*open circle*) composite film are also included

CNTs/MNPs (M: Pt, Pd, Rh and Ag) films. Wang et al. (2004) studied the impedance behaviour of $[Fe(CN)_6]^{3-/4-}$ (0.1 M KCl) on conventional gold electrode modified with colloidal gold particles. These authors reported for this composite electrode a charge-transfer resistance of $R_{ct} = 1.24$ kΩ that appears to be significantly greater compared to the charge-transfer resistance estimated in the present work on either unmodified N-MWCNTs or modified N-MWCNTs/MNPs composite films (M: Pt, Pd, Rh and Ag). Furthermore, Zhang and Oyama (2005) probed their nanostructured indium tin oxide film modified with gold nanoparticles towards $[Fe(CN)_6]^{3-/4-}$ (0.1 M PBS, pH 7.0) and reported charge-transfer resistance values lying in the range from 13.46 to 29.22 kΩ, which are considerably greater compared to those estimated in present work for the same redox system on N-MWCNTs/MNPs composite films. This comparison demonstrates that the barrier for electron transfer on N-MWCNTs/MNPs (M: Pt, Pd, Rh and Ag) appears to be significantly smaller compared to other electrodes reported in literature. It is apparent that the interfacial charge transfer occurs more easily and rapidly on our novel composite films due to the combined electrocatalytic activity of N-MWCNTs and metal nanoparticles. The results extracted from the present work exhibit exactly how important is the decoration of N-MWCNTs with metal nanoparticles for the enhancement of their electrocatalytic activity.

Conclusions

In the present work, N-MWCNTs were fabricated by means of chemical vapour deposition technique, modified with metal nanoparticles (PtNPs, PdNPs, RhNPs and AgNPs), and their electrochemical response towards the reversible redox system $[Fe(CN)_6]^{3-/4-}$ (1.0 M KCl) was investigated. In general, an improvement of electrochemical response and detection ability of composite films upon their modification with metal nanoparticles were observed. Furthermore, a strong dependence of electrochemical response and sensitivity of N-MWCNTs/MNPs on the sort of attached metal nanoparticles were recognized. Specifically, the findings demonstrate that the anodic current response and the charge-transfer kinetics of novel composite films

towards $[Fe(CN)_6]^{3-/4-}$ enhance progressively with the following order: N-MWCNTs < N-MWCNTs/RhNPs < N-MWCNTs/PdNPs < N-MWCNTs/PtNPs < N-MWCNTs/AgNPs. Likewise, the detection ability and sensitivity of composite films towards $[Fe(CN)_6]^{3-/4-}$ are improved with the same order. Specifically, the findings demonstrate an enhancement of film's sensitivity towards $[Fe(CN)_6]^{3-/4-}$ of about 29, 50, 65 and 80 % upon modification with RhNPs, PdNPs, PtNPs and AgNPs, respectively. The findings demonstrate the great influence of modification with metal nanoparticles on electrochemical response of N-MWCNTs films.

Acknowledgments The authors would like to thank Mrs. Doreen Schneider and Mrs. Sabine Heusing (Ilmenau University of Technology). The scientific work concerning the synthesis of metal nanoparticles was financially supported by BMBF-project "BactoCat" (Kz: 031A161A).

References

Attard GS, Bartlett PN, Colemen NRB, Elliott JM, Owen JR, Wang JH (1997) Mesoporous platinum films from lyotropic liquid crystalline phases. Science 278:838–840

Barreira SVP, García-Morales V, Pereira CM, Manzanares JA, Silva F (2004) Electrochemical impedance spectroscopy of polyelectrolyte multilayer modified electrodes. J Phys Chem B 108:17973–17982

Bernholc J, Brenner D, Buongiorno Nardelli M, Meunier V, Roland C (2002) Mechanical and electrical properties of nanotubes. Annu Rev Mater Res 32:347–375

Brahman PK, Dar RA, Tiwari S, Pitre KS (2012) Electrochemical behavior of gatifloxacin at multi-walled carbon nanotube paste electrode and its interaction with DNA. Rev Anal Chem 31:83–92

Burda C, Chen X, Narayanan R, El-Sayed MA (2005) Chemistry and properties of nanocrystals of different shapes. Chem Rev 105:1025–1102

Chung HT, Won JH, Zelenay P (2013) Active and stable carbon nanotube/nanoparticle composite electrocatalyst for oxygen reduction. Nat Commun 4:1922. doi: 10.1038/ncomms2944

Doron A, Katz E, Willner L (1995) Organization of Au colloids as monolayer films onto ITO glass surfaces: application of the metal colloid films as base interfaces to construct redox-active monolayers. Langmuir 11:1313–1317

Dumitrescu I, Unwin PR, Macpherson JV (2009) Electrochemistry at carbon nanotubes: perspective and issues. Chem Commun 45:6886–6901

Galus Z (1994) Fundamentals of electrochemical analysis, 2nd edn. Ellis Horwood, New York, p 257

He H, Xie Q, Zhang Y, Yao S (2005) A simultaneous electrochemical impedance and quartz crystal microbalance study on antihuman immunoglobulin G adsorption and human immunoglobulin G reaction. J Biochem Biophys Methods 62:191–205

Hirano A, Kanai M, Nara T, Sugawara M (2001) A glass capillary ultramicroelectrode with an electrokinetic sampling ability. Anal Sci 17:37–43

Jarvi TD, Sriramulu S, Stuve EM (1997) Potential dependence of the yield of carbon dioxide from electrocatalytic oxidation of methanol on platinum(100). J Phys Chem B 101:3649–3652

Knauer A, Köhler JM (2013) Screening of multiparameter spaces for silver nanoprism synthesis by microsegmented flow technique. Chem Ing Tech 85:467–475

Knauer A, Thete A, Li S, Romanus H, Csaki A, Fritzsche W, Köhler JM (2011) Au/Ag/Au double shell nanoparticles with narrow size distribution obtained by continuous micro segmented flow synthesis. Chem Eng J 166:1164–1169

Knauer A, Csaki A, Möller F, Hühn C, Fritzsche W, Köhler JM (2012) Microsegmented flow-through synthesis of silver nanoprisms with exact tunable optical properties. J Phys Chem C 116:9251–9258

Köhler JM, Li S, Knauer A (2013) Why is micro segmented flow particularly promising for the synthesis of nanomaterials? Chem Eng Technol 36:887–899

Konopka SJ, McDuffie B (1970) Diffusion coefficients of ferri- and ferrocyanide ions in aqueous media, using twin-electrode thin-layer electrochemistry. Anal Chem 42:1741–1746

Li Y, Chen SM (2012) The Electrochemical properties of acetaminophen on bare glassy carbon electrode. Int J Electrochem Sci 7:2175–2187

Liu S, Tang Z, Wang E, Dong S (2000) Electrocrystallized platinum nanoparticle on carbon substrate. Electrochem Commun 2:800–804

Lu Q, Hu S, Pang D, He Z (2005) Direct electrochemistry and electrocatalysis with hemoglobin in water-soluble quantum dots film on glassy carbon electrode. Chem Commun 20:2584–2585

Luo H, Shi Z, Li N, Gu Z, Zhang Q (2001) Investigation of the electrochemical and electrocatalytic behavior of single-wall carbon nanotube film on a glassy carbon electrode. Anal Chem 73:915–920

Musamech M, Wang J, Merkoci A, Lin YH (2002) Low-potential stable NADH detection at carbon-nanotube-modified glassy carbon electrodes. Electrochem Commun 4:743–746

Nicholson R (1965) Theory and application of cyclic voltammetry for measurement of electrode reaction kinetics. Anal Chem 37:1351–1355

Niranjana E, Swamy BEK, Naik RR, Sherigara BS, Jayadevappa H (2009) Electrochemical investigations of potassium ferricyanide and dopamine by sodium dodecyl sulphate modified carbon paste electrode: a cyclic voltammetric study. J Electroanal Chem 631:1–9

Pandurangachar M, Swamy BEK, Chandrashekar BN, Gilbert O, Reddy S, Sherigara BS (2010) Electrochemical investigations of potassium ferricyanide and dopamine by 1-butyl-4-methylpyridinium tetrafluoro borate modified carbon paste electrode: a cyclic voltammetric study. Int J Electrochem Sci 5:1187–1202

Pauliukaite R, Ghica ME, Fatibello-Filho O, Brett CMA (2010) Electrochemical impedance studies of chitosan-modified electrodes for application in electrochemical sensors and biosensors. Electrochim Acta 55:6239–6247

Perenlei G, Tee TW, Yusof NA, Kheng GJ (2011) Voltammetric detection of potassium ferricyanide mediated by multi-walled carbon nanotube/titanium dioxide composite modified glassy carbon electrode. Int J Electrochem Sci 6:520–531

Roto R, Villemure G (2002) Electrochemical impedance spectroscopy of electrodes modified with thin films of Ni/Al/Cl layered double hydroxides. J Electroanal Chem 527:123–130

Szroeder P, Tsierkezos NG, Scharff P, Ritter U (2010) Electrocatalytic properties of carbon nanotube carpets grown on Si-wafers. Carbon 48:4489–4496

Talapin DV, Lee JS, Kovalenko MV, Shevchenko EV (2010) Prospects of colloidal nanocrystals for electronic and optoelectronic applications. Chem Rev 110:389–458

Tsierkezos NG, Ritter U (2010) Electrochemical impedance spectroscopy and cyclic voltammetry of ferrocene in acetonitrile/acetone system. J Appl Electrochem 40:409–417

Tsierkezos NG, Ritter U (2011) Determination of impedance spectroscopic behaviour of triphenylphosphine on various electrodes. Anal Lett 44:1416–1430

Tsierkezos NG, Ritter U (2012) Electrochemical responses and sensitivities of films based on multi-walled carbon nanotubes in aqueous solutions. J Solut Chem 41:2047–2057

Wang J, Agnes L (1992) Miniaturized glucose sensors based on electrochemical codeposition of rhodium and glucose oxidase onto carbon-fiber electrodes. Anal Chem 64:456–459

Wang L, Wang E (2004) Direct electron-transfer between cytochrome c and a gold nanoparticles modified electrode. Electrochem Comm 6:49–54

Wang M, Wang L, Yuan H, Ji X, Sun C, Ma L, Bai Y, Li T, Li J (2004) Immunosensors based on layer-by-layer self-assembled Au colloidal electrode for the electrochemical detection of antigen. Electroanalysis 16:757–764

Xiao Y, Patolsky F, Katz E, Hainfeld JF, Willner I (2003) Plugging into enzymes: nanowiring of redox enzymes by a gold nanoparticle. Science 299:1877–1881

Xu X, Jiang S, Hu Z, Liu S (2010) Nitrogen-doped carbon nanotubes: high electrocatalytic activity toward the oxidation of hydrogen peroxide and its application for biosensing. ACS Nano 4:4292–4298

Yu J, Zhao J, Hu C, Hu S (2007) Enhanced oxidation of estrone at multi-wall carbon nanotubes film electrode: direct evidence for the advantage of carbon nanotubes over other carbonaceous materials. J Nanosci Nanotechnol 7:1631–1638

Zhang J, Oyama M (2005) Gold nanoparticle arrays directly grown on nanostructured indium tin oxide electrodes: characterization and electroanalytical application. Anal Chim Acta 540:299–306

Zhao Q, Gan Z, Zhuang Q (2002) Electrochemical sensors based on carbon nanotubes. Electroanalysis 14:1609–1613